Climate change impact assessment on potential rubber cultivating area in the Greater Mekong Subregion

To cite this article before publication: Reza Golbon *et al* 2018 *Environ. Res. Lett.* in press https://doi.org/10.1088/1748-9326/aad1d1

Climate change impact assessment on potential rubber cultivating area in the Greater Mekong Subregion

Authors

Reza Golbon, Marc Cotter, Joachim Sauerborn

University of Hohenheim, Institute of Agricultural Sciences in the Tropics (Hans-Ruthenberg-Institute), Agroecology in the Tropics and Subtropics

Address: Garbenstr. 13, 70599, Stuttgart, Germany

E-mail: golbon@uni-hohenheim.de

Abstract

In order to map potential shifts of rubber (*Hevea brasiliensis*) cultivation as a consequence of the ongoing climate change in the Greater Mekong Subregion, we applied rule-based classifications to a selection of nine gridded climatic data projections (precipitation and temperature, Global Circulation Models (GCMs)). These projections were used to form an ensemble model set covering the Representative Concentration Pathways (RCPs) 4.5 and 8.5 of the Fifth Assessment Report of the Intergovernmental Panel on Climate Change at three future time sections: 2030, 2050 and 2070. We used a post classification ensemble formation technique based on majority outcome of the classification to not only provide an ensemble projection but also to spatially track and weight the disagreements between the classified GCMs. A similar approach was used to form an ensemble model aggregating the involved climatic factors. The level of parsimony between the ensemble projections and GCM products was assessed for each climatic factor separately, and also at the aggregate level. Shifting zones with high confidence were clustered based on their land use composition, physiographic attributes and proximity. Following the same ensemble formation technique and by setting a 28°C threshold for annual mean temperature, we mapped areas prone to exposure to potentially excessive heat levels. Almost the entire shift projected with high certainty was in form of expansion, associated with temperature components of climate and temporally limited to the 2030 time window where the total area conducive to rubber cultivation in the GMS is projected to exceed 50% by 2030 (from 44.3% at the turn of the century). The largest detected cluster (41% of the total shifting area), which also is the most ecologically degraded, corresponds to Northern Vietnam and Guangxi Autonomous Region of China. The area exposed to potentially excessive heat is projected to undergo a 25-fold increase under RCP4.5 by 2030 from 14568 km^2 at the baseline.

Keywords

Multi-model ensemble, mapping of rubber, Para rubber tree, cash crops, geographic information systems, biodiversity, deforestation, Mekong Region, Mainland Southeast Asia

Introduction

Natural rubber is a key industrial commodity with wide application in manufacturing of a very diverse range of products. Although rubber-bearing plant species such as *Taraxacum kok-saghyz* and *Parthenium argentatum* have lately reemerged on the research and development scene as potential alternative sources of natural rubber (van Beilen and Poirier 2007a, 2007b, Rasutis *et al* 2015, Kreuzberger *et al* 2016, Dong *et al* 2017, Ramirez-Cadavid *et al* 2107, Soratana *et al* 2017), the Para rubber tree *(Hevea brasiliensis)* has retained its status as the sole viable source of natural rubber, which does not seem to change in the close future (Cornish 2017). Global consumption of natural rubber has exceeded 12 million metric tons in the last three years according to the International Rubber Study Group (IRSG 2017). Raising demand has been matched and to some extent surpassed by increases in production. Global trends of the natural rubber production and consumption and the harvested area are illustrated in figure 1.

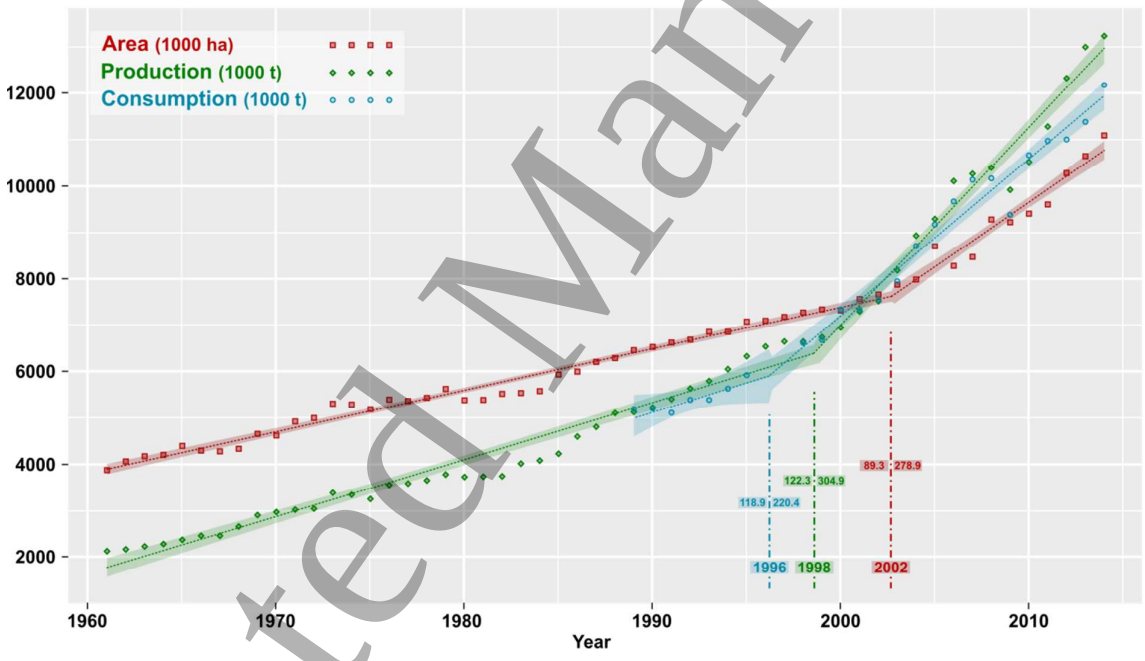

Figure 1 Global trends for consumption, production and area under rubber cultivation
Segmented regression lines reveal the shifts in trends: 1996 is the estimated year before which a 118.9 thousand ton increase per year explained the growing consumption trend, accelerating to 220.4 thereafter while for production, the slope has shifted from 122.3 to 304.9 thousand tons per year by 1998 and year 2002 appears to be the most efficient breakpoint explaining the increasing trend of the global area under rubber cultivation, surging from 89.3 to 287.9 thousand hectares added each year. We have used R package 'segmented' (Muggeo 2003) version 0.5-1.4 to generate this figure from FAOSTAT (production and area) and IRSG (consumption) data (FAOSTAT 2017, IRSG 2017). Inkscape 0.91 was used for visual optimization.

Recent decades have been associated with expansion (and to some extent shift) of rubber cultivation zones from the traditional rubber growing regions (the 10°S to 10°N equatorial belt) to higher latitudes and longitudes (Priyadarshan *et al* 2005, Ziegler *et al* 2009, Li and Fox 2012, Ahrends *et al* 2015, Chen *et al* 2016a, Chen *et al* 2016b). Thailand, the leading rubber producing country since 1990, which also has had the highest share of the global area converted each year to rubber cultivation (30% on average since the turn of the century), can well illustrate the situation (figure 2).

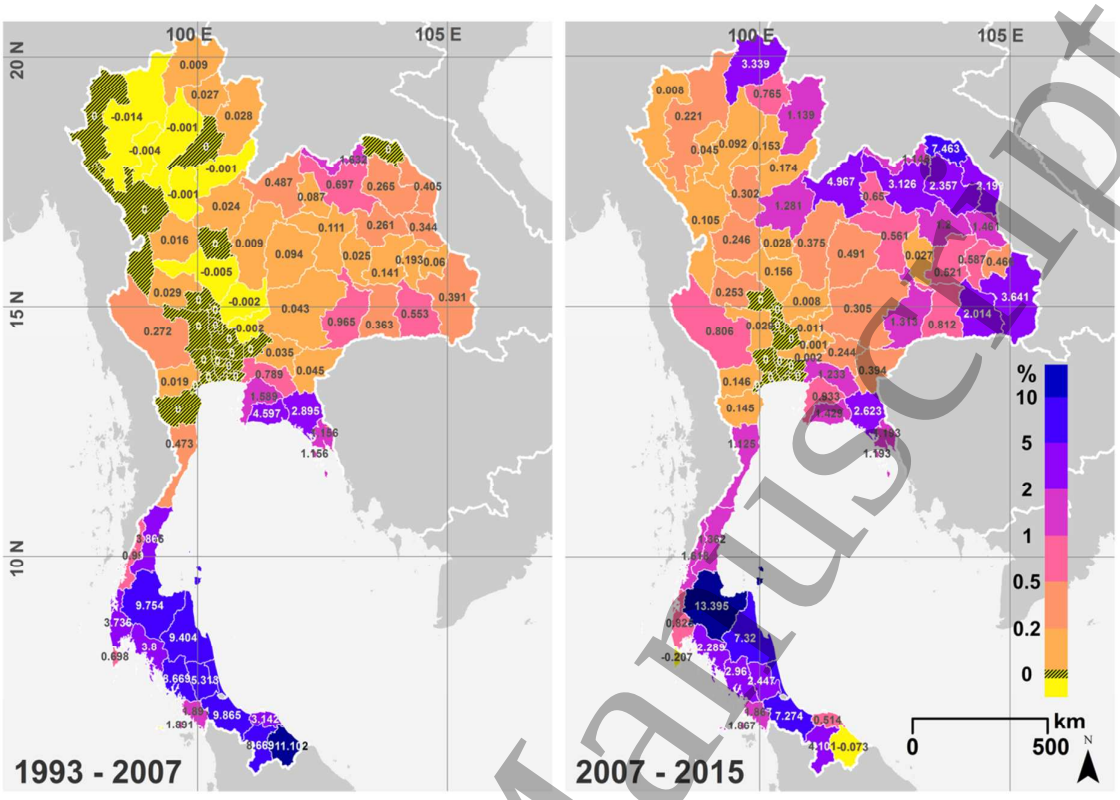

Figure 2 Temporal dynamics of the expansion of rubber cultivation in Thailand
The provincial share of the Thai national increase in the area under rubber cultivation in two time sections: from 1993 to 2007 (3158 km^2) and from 2007 to 2015 (12485 km^2). The 1993 Thailand Agricultural Census (NSO 1994) and the agricultural statistics yearbooks of Thailand (2009 and 2015) data (available at www.oae.go.th) and the GADM administrative divisions' shapefiles (2.8) were used. Maps were generated in ArcGIS 10.2.2 and visually optimized in Inkscape 0.92.

The Greater Mekong Subregion (GMS) is an economic cooperation program consisting of six nations: China (Yunnan province and Guangxi autonomous region), Vietnam, Thailand, Laos, Myanmar and Cambodia. The GMS covers more than 2.5 million km^2 of the Mainland Southeast Asia (MSEA), about 84% of which overlaps with the Indo-Burmese mega biodiversity hotspot (Myers *et al* 2000, Mittermeier *et al* 2004, figure 3). It stands for a substantial share of global rubber production (46.7% in 2014)[1] almost exclusively coming from monocultures. Since its inception in the early 1990s, the GMS has in general, and its formerly isolated members (Myanmar, Laos and Cambodia) in particular, been undergoing rapid socio-economic change through regional development programs and transboundary investments in all conceivable sectors. At the same time, ecological degradation through accelerated landscape transformation has been observed. Heavy expansion of rubber monocultures and their spread to new areas have had a notable contribution to deforestation, habitat

[1] This figure is mainly based on FAOSTAT data. As two Chinese provinces of Hainan and Guangdong contribute to the Chinese national production, their share (46.2% in 2014 as mentioned in the China Statistical Yearbook 2016 www.stats.gov.cn) has been deducted. In case of Laos for which FAO data is not available, United Nations Commodity Trade Statistics Data (comtrade.un.org) was used in combination with the historical commodity prices (www.indexmundi.com) to estimate the national rubber production: 56 thousand tons.

fragmentation and biodiversity loss (Li *et al* 2007, Ahrends *et al* 2015, He and Martin 2015, Häuser *et al* 2015).

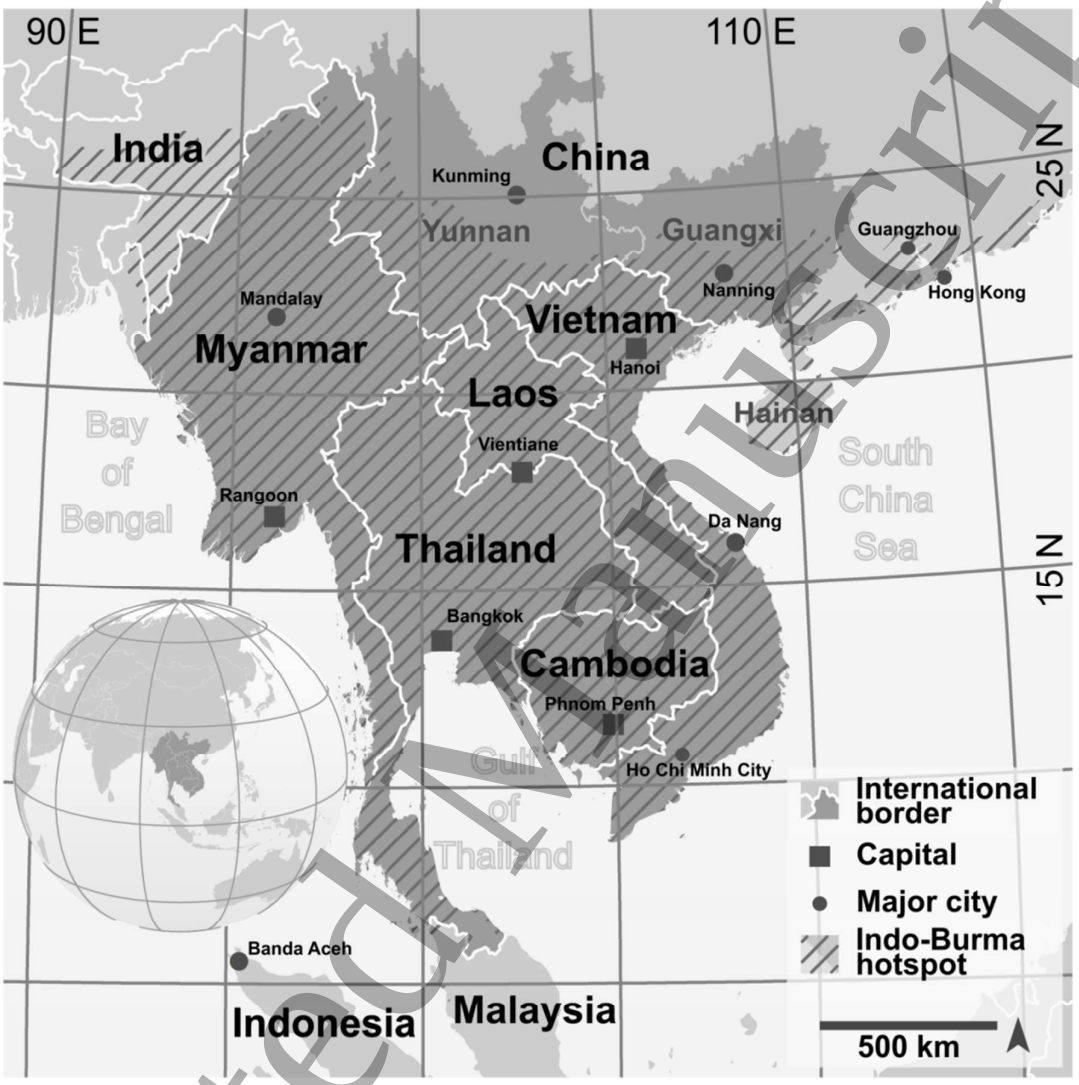

Figure 3 Geographical extent covered by this study
The Greater Mekong Subregion (dark gray area) is the spatial extent covered in this study. The GADM administrative divisions' shapefiles 2.8 (available at www.gadm.org) and the CEFP biodiversity hotspots shapefiles based on Myers *et al* (2000) and Mittermeier *et al* (2004) (available at www.cepf.net) were used to generate the map in ArcGIS 10.2.2 (visually optimized in Inkscape 0.92).

In response to concerns about the ecological implications of the rapid expansion of rubber monocultures mostly replacing forests and swidden agriculture in MSEA, remote sensing techniques are regularly used to monitor land use conversion to rubber cultivation (e.g. Li and Fox 2011a, 2011b, 2012, Dong *et al* 2012, 2013, Senf *et al* 2013, Fan *et al* 2015, Grogan *et al* 2015, Li *et al* 2015, Chen *et al* 2016a, 2016b, Kou *et al* 2017). More recently, remote sensing has been used to track additional details such as the rubber plantation age (Koedsin and Huete 2015, Kou *et al* 2015, Beckschäfer 2017, Trisasongko 2017).

Climate is one of the defining factors of the potential geographic extent for cultivation of any crop, and Para rubber is no exception. Momentous ongoing change in Earth's climate attributed to human activity (Collins *et al* 2013, Power *et al* 2013, Lewandowsky *et al* 2016, Thorne 2017, Medhaug *et al* 2017, Berger *et al* 2017) is comprehensively acknowledged by the scientific community (Cook *et al* 2016). Some forecasts of the future potential geographical range for Para rubber in different parts of MSEA, mainly based on ecological niche modeling (Ray *et al* 2014a, 2014b, 2016, Ahrends *et al* 2015, Liu *et al* 2015) and bioclimatic stratification (Zomer *et al* 2014) have recently been published.

Gridded data of climatic factors simulating likely future conditions are essential inputs for forecasts. Global Circulation Models (GCMs) are useful sources of information commonly exploited to assess the potential impacts of climate change. Various institutions are engaged in creating such datasets and provide dozens of potential choices as input. Variations among GCMs, which mainly rise from structural and parameterization differences (Semenov and Stratonovitch 2010), can help to provide a means to capture and explore some of the projection uncertainties which have to be accounted for in order to obtain a realistic and scientifically sound image. Variabilities observed in sets of comparable simulations prompt some key choice questions, starting with whether a single simulation would suffice or a multi-member ensemble is needed for a reasonably robust forecast. In the latter case, can using the largest possible ensemble be a legitimate decision or could a reduced set of simulations perform better while minimizing the computational cost? Based on what criteria should a shortlisting take place? Should an average of all set members be used as ensemble or (considering the spatial nature of the data) is there a better option? How to handle the uncertainties (dispersion) inherent in the input differences (an important but so far overlooked factor)? And how to communicate these uncertainties in a comprehensive and useful way?

Potential phytosanitary deficiencies as well as growth and yield failures due to crop exposure to excessive levels of ambient temperature are some of the more unsettling aspects of climate change. Despite the existing evidence for this matter (Abd Karim 2008, Kositsup *et al* 2009, Yu *et al* 2014, Golbon *et al* 2015, Jayasooryan *et al* 2015, Nguyen and Dang 2016), setting a clear-cut threshold for heat stress is still a debatable subject.

Here, we apply rule-based geographical classification to a selection of the downscaled IPCC AR5 climatic projections in order to map the potential geographical zones projected to be climatically suitable for Para rubber cultivation, or exposed to excessive heat, in MSEA in three time sections centered on 2030, 2050 and 2070 while accounting for and presenting the classification uncertainty.

Data and methods

Data

We used the WorldClim dataset (version 1.4, Hijmans *et al* 2005) to generate the baseline climatic map and an ensemble of nine GCMs under the Fifth Assessment Report of the Intergovernmental Panel on Climate Change (IPCC AR5) as simulations forecasting the climatic conditions for three 20-year time periods centered on 2030, 2050 and 2070. Facing the choice questions mentioned in the introduction section, we referred to McSweeney *et al* (2015), which ranked IPCC AR5 GCMs according to their regional performances and recommended a subset of 8-10 GCMs, avoiding the least realistic models while retaining the maximum plausible dispersion. Nine GCMs were selected using the regional plausibility rankings: ACCESS1.0 (Bi *et al* 2013, Dix *et al* 2013), CCSM4 (Gent *et al* 2011), IPSL-CM5A-LR (Dufresne *et al* 2013), NorESM1-M (Bentsen *et al* 2013), GFDL CM3 (Donner *et al* 2011), BCC_CSM1.1 (Xin *et al* 2013), MRI-CGCM3 (Yukimoto *et al* 2012), HadGEM2-ES (Martin *et al* 2011) and MPI-ESM-LR (Giorgetta *et al* 2013). The GCM data were provided by the Climate Change and Food Security (CCAFS) Program data portal of the International Center for Tropical Agriculture (CIAT) (available at www.ccafs-climate.org) and were downscaled to 30 arc sec (~1 km) resolution using delta method (Ramirez-Villegas and Jarvis 2010). Two of the four main climate change scenarios recognized by the IPCC AR5 were considered in this study: Representative Concentration Pathways (RCPs) 8.5 and 4.5. RCP 8.5 is a high greenhouse gas (GHG) emission scenario comprising no stabilization of the atmospheric GHG concentrations leading to 8.5 Wm^{-2} of radiative forcing by 2100 and a globe over 4°C warmer than the pre-industrial era. RCP 4.5 is a moderate scenario accommodating GHG concentration stabilization by 2070 and radiative forcing of 4.5 Wm^{-2} (2.5° C temperature rise) by the end of the 21st century (Riahi *et al* 2011, Thomson *et al* 2011). Land use data (see supplementary material figure S1, Hoskins *et al* 2016), the Biodiversity Intactness Index (BII) created by Newbold *et al* (2016, supplementary material figure S2) and the USGS GTOPO30 digital elevation model were used to cluster and describe the potential future expansion/retraction zones. We have also used the administrative divisions (GADM) shapefiles (available at www.gadm.org) in this study.

Methods

Five climatic suitability criteria adapted from Rivano *et al* (2015) listed in table 1 were used in this study. As mentioned by Thompson *et al* (2013) and Stephens *et al* (2012) it is essential to avoid averaging for ensemble formation as it leads to information loss on variation. Here we conducted the complete classification process on the involved gridded variables separately for each GCM and formed the ensemble product by the majority outcome for each grid cell overlaid with a simple uncertainty measure reflecting the strength of the majority. The total annual precipitation and the mean annual temperature layers were directly categorized to optimal, suboptimal and prohibitive ranges for each GCM, time section and scenario. The ensemble suitability projections were generated for each

'criterion × time section × scenario' combination consisting of the suitability class returned by the majority of the GCMs for every grid cell and a corresponding uncertainty layer reflecting the strength of the consensus on the class assigned to each ensemble grid cell ranging from full agreement (9/9) to mere majority (5/9). The monthly mean temperature and the monthly precipitation gridded data went through a similar process with two additional steps (see figure 4), summarizing the intra-annual distribution of precipitation and temperature.

Table 1 Criteria and thresholds for classification of the gridded climatic data

Climatic criterion	Range			
	Prohibitive	**Suboptimal**	**Optimal**	**Excessive**
Annual mean temperature (°C)	< 23	23-25	25-28	> 28
Number of months with mean temperature below 23°C	> 5	1-5	0	-
Annual precipitation (mm)	< 1100	1100-1500	> 1500	-
Number of months with precipitation below 50mm	> 5	4-5	0-3	-

Thresholds used in this study are adapted from Rivano *et al* (2015). The number of months with mean temperature below 23°C is referred to as intra annual temperature distribution and the number of months with precipitation below 50mm as intra annual precipitation distribution.

By overlaying the classification outcomes of the climatic layers, each grid cell was assigned one of the following summarizing classes: 'AllOpt' where all climatic layers returned an optimal classification, 'SubOpt' where at least one layer was described as suboptimal and none as prohibitive, 'SingProh' where only one layer was in prohibitive range and 'MultProh' with more than one climatic criterion in the prohibitive range. The aggregate uncertainty layers were also overlaid to produce an aggregate uncertainty layer in four levels: 1) full agreement among GCMs for all four criteria, 2) only one criterion projected with 7 or 8 from 9 majority (and all other criteria possessing stronger consensus), 3) only one criterion projected with 5 or 6 from 9 majority (and stronger consensus in all other criteria) and 4) two or more criterion projected with 5 or 6 from 9 majority.

A point shapefile representing grid cells in the raster data was created for the shift zones with high aggregate certainty (levels 1 and 2) to which the corresponding land use, BII, altitude, slope, longitude and latitude values both in original and standardized form were extracted. We used the Grouping Analysis tool of the ArcGIS 10.2.2 to form clusters based on the standardized attributes and illustrated the outcome using 'ggplot2' 2.1.0 package in R.

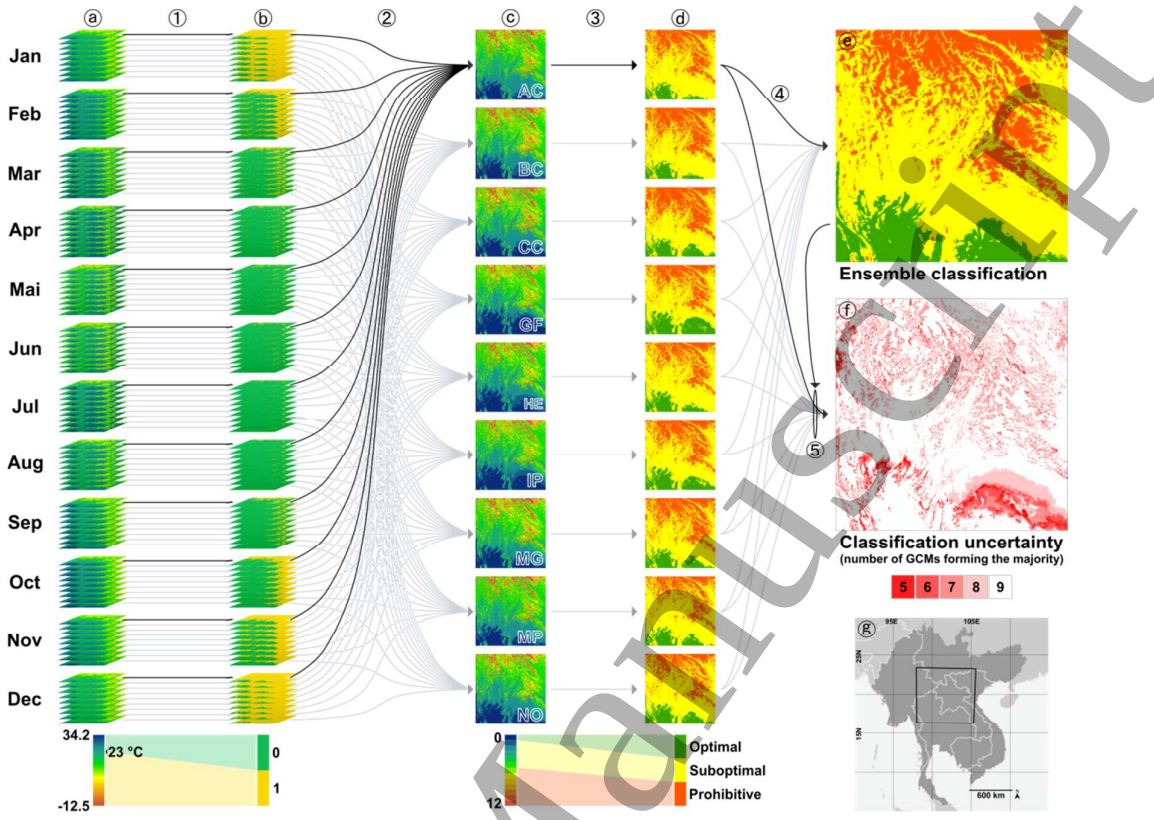

Figure 4 Steps involved in intra-annual temperature distribution suitability classification (as illustration case)

Continuous monthly mean temperature gridded data (Representative Concentration Pathway 4.5 for the 20 year period centered on 2030) ⓐ were used to generate binary layers ⓑ by setting a stress threshold ① (23° C). All 12 binary layers originating from the same Global Circulation Model (GCM) were summed ② to produce the layers reflecting the number of months projected to be below the threshold ⓒ (abbreviations AC to NO denote the corresponding GCMs). These layers were reclassified ③ to three levels: optimal, suboptimal and prohibitive ⓓ. The ensemble classification map ⓔ was generated by extracting the majority outcome of all GCMs for each grid cell ④. The uncertainty layer ⓕ reflects the consensus level among GCMs leading to the ensemble and was produced by counting the number of GCMs participating in the formation of the majority for each given grid cell ⑤. Panel ⓖ shows the geographic extents of the frame selected for illustration. All layers used in each step were assigned equal weights and the arrow color difference is only for visual clarity. ArcGIS 10.2.2 and Inkscape 0.91 were used for generation of this figure.

Sankey diagrams are illustration tools suitable for description of multidimensional and hierarchical categorical data and are most often used to show material or energy flows through network systems. Geographical classification dynamics over time can also be very efficiently presented by Sankey diagrams. As demonstrated by Cuba (2015), Sankey diagrams are superior to cross-tabulation matrices in reflecting land use dynamics, particularly when multiple time sections are of interest. We generated Sankey diagrams to illustrate the climatic suitability class shifts projected to occur under RCP 4.5 and RCP 8.5 for each adjacent pair of time sections using the D3.js JavaScript library developed by Bostock *et al* (2011).

Using the ensemble formation technique, we created an 'excessive heat' layer distinguishing the area associated with annual mean temperature exceeding 28°C at the baseline and traced its potential expansion under the two RCPs overlaid with corresponding uncertainty layers. This criterion,

however, was not used as an upper limit for transition to suboptimal or prohibitory conditions in the former steps.

Results

Single criterion classification

Climatic conditions in the study area at the baseline and the ensemble projections for the four climatic criteria (separately classified) are presented in Figures 5 and 6. Largest projected shifts (expressed as proportion of the total studied area) are observed for the annual mean temperature and the intra-annual temperature distribution moving from baseline to the 20 year time window centered on 2030. Considering the annual mean temperature, 25.13 % of the total area (642416 km^2 from 2556370 km^2) is projected (21.79 % projected with full GCM consensus) to migrate from prohibitive and suboptimal range to classes more conducive to rubber cultivation under RCP 4.5. The RCP 8.5 ensemble projection suggests this figure to be 28.55 % (23.38 % with full agreement). For intra-annual temperature distribution, 20.18 % (16.59 % with full agreement) of the total area is observed to experience such a transition under RCP 4.5 and 23.96 % (17.67 %) under RCP 8.5 from baseline to the 2030 period. Moving to 2050 and 2070 time periods, the emerging more suitable areas regarding the two aforementioned factors are of much smaller size and paired with higher degrees of uncertainty. The persistence of the new conditions in an area which has gone through climatic shift is relevant but not necessarily traceable in Sankey diagrams (Figure 5). Considering annual mean temperature under RCP 4.5, 14.17 % of the total area is projected with high certainty to remain in the new class after shifting from prohibitive to suboptimal or suboptimal to optimal range and 16.58 % under RCP 8.5. For the intra-annual temperature distribution, these figures are projected to be 14.17 % and 16.55 % respectively. Unlike temperature components of climate, the projected shifts observed in precipitation components were bilateral, associated with low certainty (i.e. high disagreement among GCMs) and smaller in size. The largest area projected to experience shifts in the precipitation class by 2030 was observed for intra-annual precipitation distribution summing to 7.02 % of the total investigated area (6.01 % moving from prohibitive to suboptimal or suboptimal to optimal and 1.01 % vice versa). 80.63 % of it (equal to 5.66% of the total area) has been projected by mere majority (i.e. the lowest possible certainty level).

Comparing single criterion GCM projections with their corresponding ensembles (Table 2) reveals that ACCESS1.0 has returned the closest single criterion maps to the ensemble with an average overlap of 92.42 % across all 24 possible criterion-RCP-time period combinations followed by BCC_CSM1.1, MPI-ESM-LR and CCSM4.

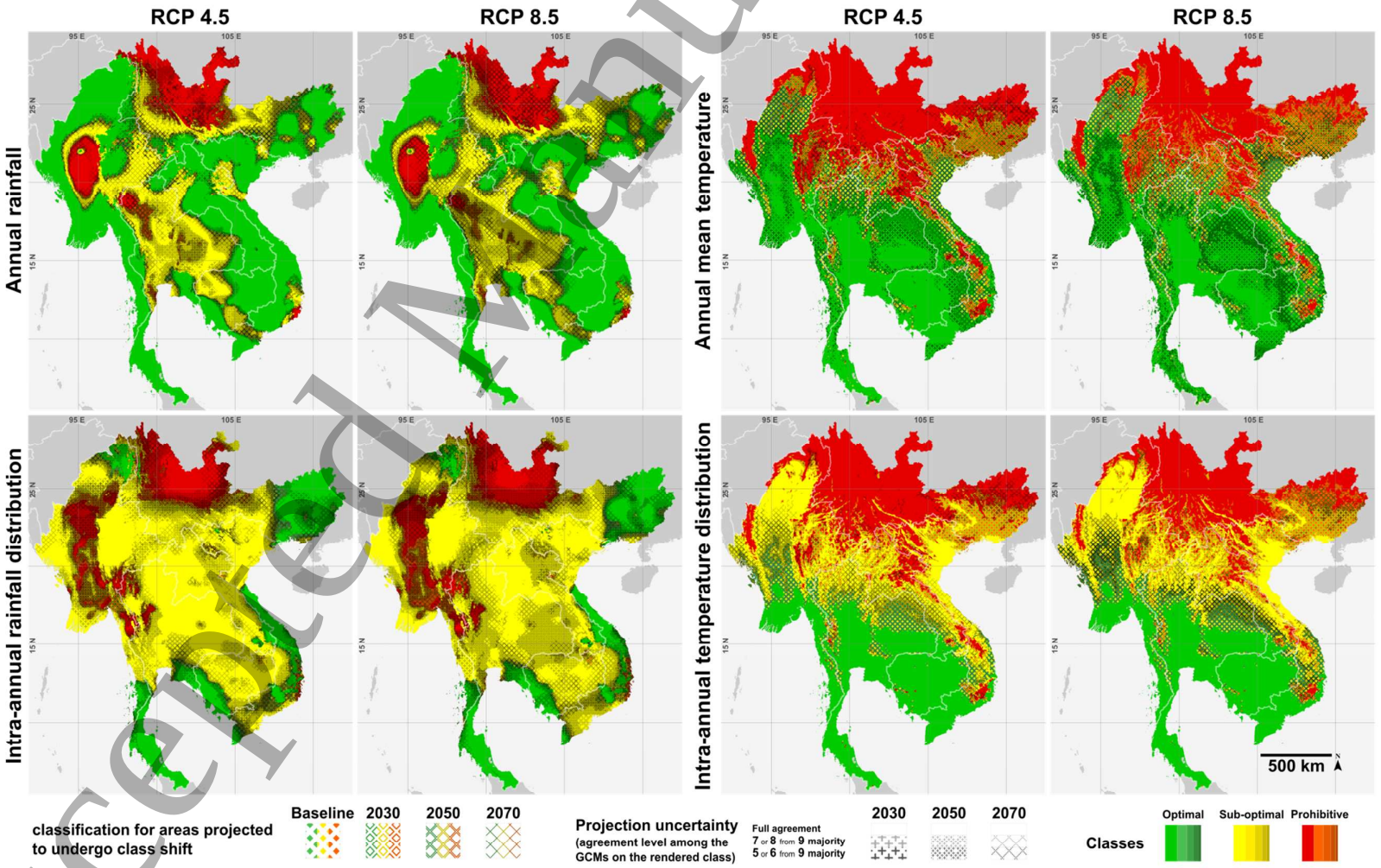

Figure 5 Baseline and projected single criterion climatic class dynamics maps

The classification dynamics for the climatic criteria considered in this study cover baseline and the ensemble future projections. Each panel contains seven (1+3+3) layers of information: suitability class at the baseline (×1), projected class shifts between the four time sections (×3), and the strength of the ensemble majority suggesting the change/no-change (×3). Please view this figure in original resolution and consult the usage guide provided in the supplementary material (figure S10) for clarifications. Maps were generated in ArcGIS 10.2.2 and visually optimized in Inkscape 9.2.

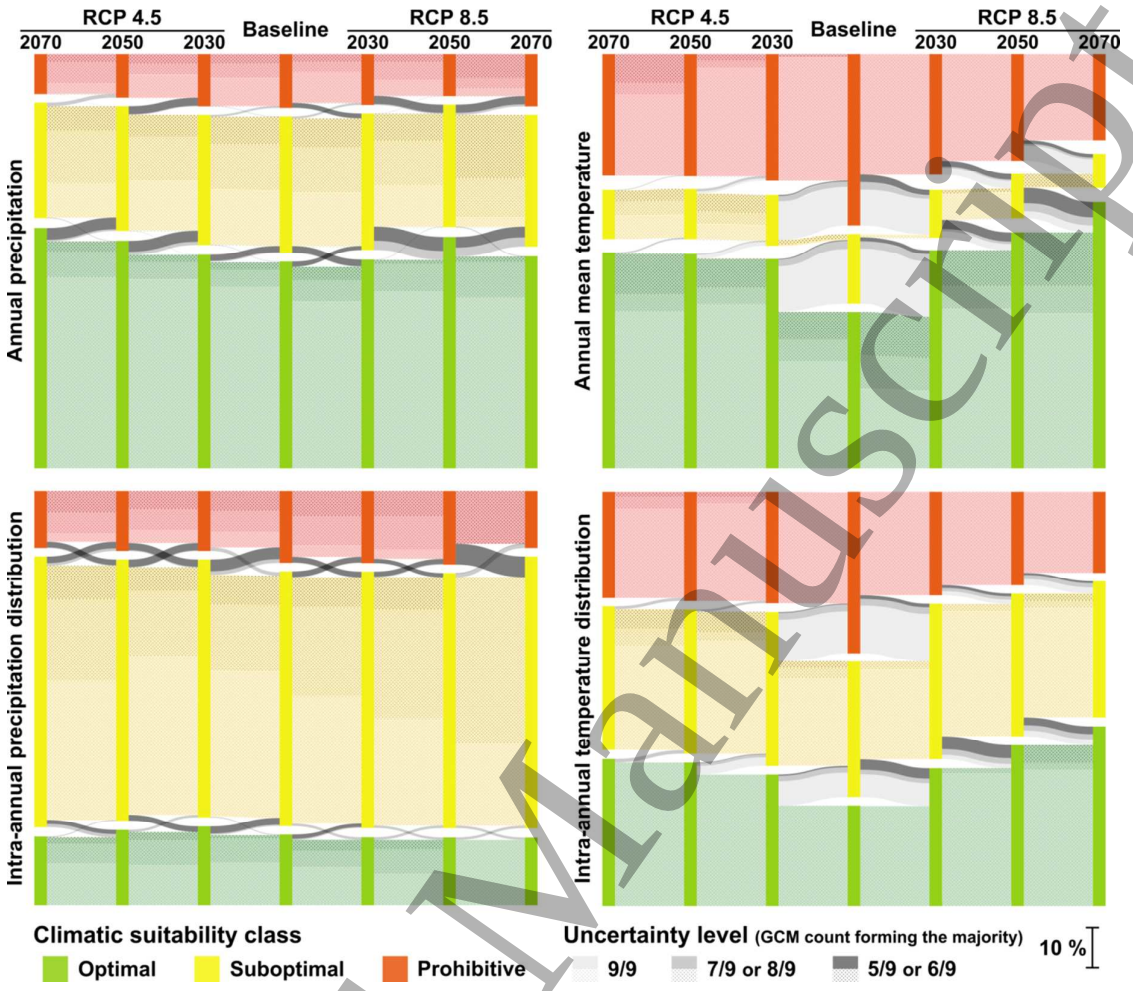

Figure 6 Baseline and projected single criterion climatic class dynamics
The classification dynamics for the area associated with the climatic criteria considered in this study at the baseline (2000) and the ensemble future projections correspond to the maps presented in figure 5. For more details on the use of Sankey diagrams in illustration of geographic shifts, view the dedicated article: Cuba (2015). Sankey charts were produced in D3.js JavaScript library (Bostock *et al* 2011) and visually optimized in Inkscape 9.2.

Aggregate classification

The geographical and temporal dynamics of the projected climatic suitability classes at the aggregate level are illustrated in figures 7 and 8. The area projected to retain its aggregate climatic class across the investigated time span (by 2070) is projected to be 72.83% of the total area under RCP 4.5 and 66.23% under RCP 8.5. By the time window centered on 2050 these projections sum to 74.98% and 72.89% and by 2030 to 77.63% and 78.22% of the total area respectively. From the total projected class-shifting area by 2030, 26.78% (6.01% of the studied area) was projected with maximum certainty (i.e. full agreement among GCMs in all four criteria) under RCP 4.5 and 26.50% (5.77%) under RCP 8.5. It was projected to decline to 14.09% (3.53%) and 17.39% (4.71%) for the baseline to 2050 time period and further reduction to 9.49% (2.58%) and 7.10% (2.40%) for 2070 respectively. Performance similarity of single GCM aggregate classification maps with the ensemble is presented in table 3 where ACCESS1.0 returned the closest results to the ensemble.

Table 2 Classification agreement between the single criterion climatic data simulations and their ensemble

Criteria	RCP	Period	Climatic data simulations								
			AC	BC	MP	CC	NO	MG	IP	HE	GF
Annual precipitation	4.5	2030	93.9	91.2	93.7	89.6	89.8	90.3	94.7	88.1	85.8
		2050	93.7	94.6	91.5	91.7	89	89.1	90.1	90.7	88.0
		2070	92.6	85.7	91.1	93.8	83.2	92.8	90.5	86.7	91.7
	8.5	2030	94.0	88.7	91.1	88.8	88.8	89.7	92.7	88.5	84.6
		2050	93.2	92.7	90.0	92.2	90.6	87.6	89.1	88.1	84.7
		2070	89.2	84.1	88.6	89.6	85.9	92.5	87.2	83.2	89.1
Intra-annual precipitation distribution	4.5	2030	90.5	85.0	91.0	84.7	89.5	92.6	88.2	92.5	79.1
		2050	91.1	88.6	87.8	87.0	89.6	90.7	86.3	87.7	85.4
		2070	90.4	81.1	89.2	89.7	84.5	87.3	87.1	89.2	87.1
	8.5	2030	92.4	87.2	90.6	88.0	89.3	83.6	75.2	88.2	86.3
		2050	92.6	83.3	90.7	88.1	79.4	91.6	72.5	83.3	88.0
		2070	91.7	87.5	86.2	86.4	81.9	87.9	64.7	84.0	82.5
Annual average temperature	4.5	2030	91.5	99.2	82.3	91.3	92.2	90.3	87.5	90.1	86.4
		2050	91.2	99.3	89.0	91.9	93.6	88.7	88.6	85.4	80.8
		2070	81.5	99.2	86.4	95.9	92.8	90.7	86.3	73.2	77.0
	8.5	2030	96.6	96.5	97.8	92.2	87.3	85.0	90.2	89.5	93.4
		2050	91.6	95.7	98.8	90.3	89.1	80.7	86.9	85.5	87.8
		2070	92.1	93.7	98.6	86.2	85.5	78.0	87.6	80.6	89.7
Intra-annual temperature distribution	4.5	2030	97.0	96.1	92.4	98.2	96.1	95.0	94.7	96.7	94.0
		2050	96.0	96.5	92.2	97.4	96.4	93.3	96.0	93.3	90.8
		2070	90.5	96.6	92.1	97.7	96.1	92.8	95.2	86.8	88.8
	8.5	2030	95.7	95.8	97.0	98.6	94.7	93.6	96.5	93.9	96.7
		2050	94.6	93.5	97.3	96.1	94.3	89.9	96.1	92.3	93.7
		2070	94.4	95.2	98.7	94.7	93.5	88.9	96.4	91.1	95.6

Resemblance of the climatic classification by each of the nine simulations used in this study with their ensemble is expressed as proportion (%) of the sum of the areas with matching classification to the total area. Color-code reflects five levels: below 75%, 75 - 90%, 90.1 - 95%, 95.1 - 99% and above 99%. Maximum and minimum of each row are underlined. Nine IPCC AR5 simulations of representative concentration pathways RCP 4.5 and RCP 8.5 were used, here abbreviated as AC: ACCESS1.0 (Bi *et al* 2013, Dix *et al* 2013), CC: CCSM4 (Gent *et al* 2011), IP: IPSL-CM5A-LR (Dufresne *et al* 2013), NO: NorESM1-M (Bentsen *et al* 2013), GF: GFDL CM3 (Donner *et al* 2011), BC: BCC_CSM1.1 (Xin *et al* 2013), MG: MRI-CGCM3 (Yukimoto *et al* 2012), MP: MPI-ESM-LR (Giorgetta *et al* 2013) and HE: HadGEM2-ES (Martin *et al* 2011). Each time period corresponds to a 20 year (averaged) time section centered on the mentioned year. GCMs are rank-sorted from left to right by their overall resemblance to ensemble.

Restricting the investigated time window to the 20 year period centered on 2030 and the area to where climatic conditions are projected with high (the upper two levels) certainty to shift from prohibitive to rubber cultivation to suboptimal or optimal, our projections detected 195928 km^2 (7.70% of the total investigated area) under RCP 4.5 and 238734 km^2 (9.38%) under RCP 8.5 which are presented in Figure 8. Using Grouping Analysis we detected eight major clusters based on land use composition, physiographic attributes and proximity. Northernmost potential expansion was projected to verge on 27°N of the Irrawaddy basin and the altitudinal limit to exceed 1400 m a.s.l. in clusters 7 (Bilauktaung range Thailand-Myanmar border between 15.56 °N and 18.10 °N) and 8 (Cardamom Mountains of Cambodia) (Figure 9). The overall baseline state of biodiversity in these clusters is presented in figure 10 using the biodiversity intactness index (BII). Steffen *et al* (2015) have proposed a safe limit value of 0.9 (maximum 10% decline) for BII. The largest cluster (cluster 1) corresponding to Guangxi Autonomous Region of China and Northern Vietnam is the most ecologically degraded and accommodates 92.47% of the area already below the safe threshold.

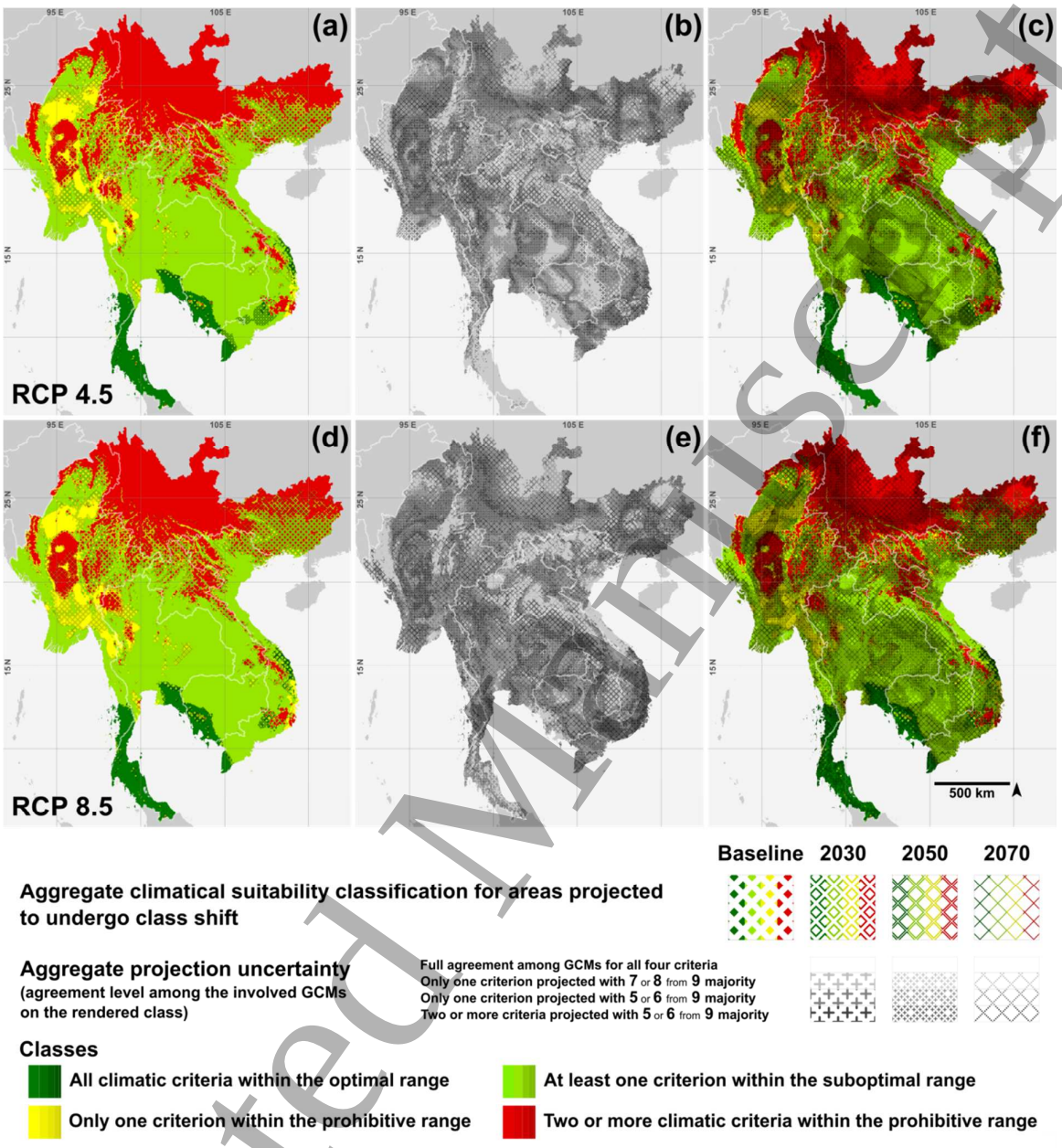

Figure 7 Aggregate climatic classification maps

Panels (a) and (d) reflect four (1+3) layers of information: the aggregate suitability class at the baseline (×1) and the projected class shifts between the four time sections (×3). Panels (b) and (e) demonstrate the strength of the ensemble majority suggesting the change/no-change (×3) between temporally adjacent time sections. Aggregate classification layers (a) and (d), and the corresponding uncertainty layers (b) and (e) are overlaid to produce panels (c) and (f). Please view this figure in original resolution and consult the usage guide provided in the supplementary material (figure S10) for clarifications. Maps were generated in ArcGIS 10.2.2 and visually optimized in Inkscape 9.2.

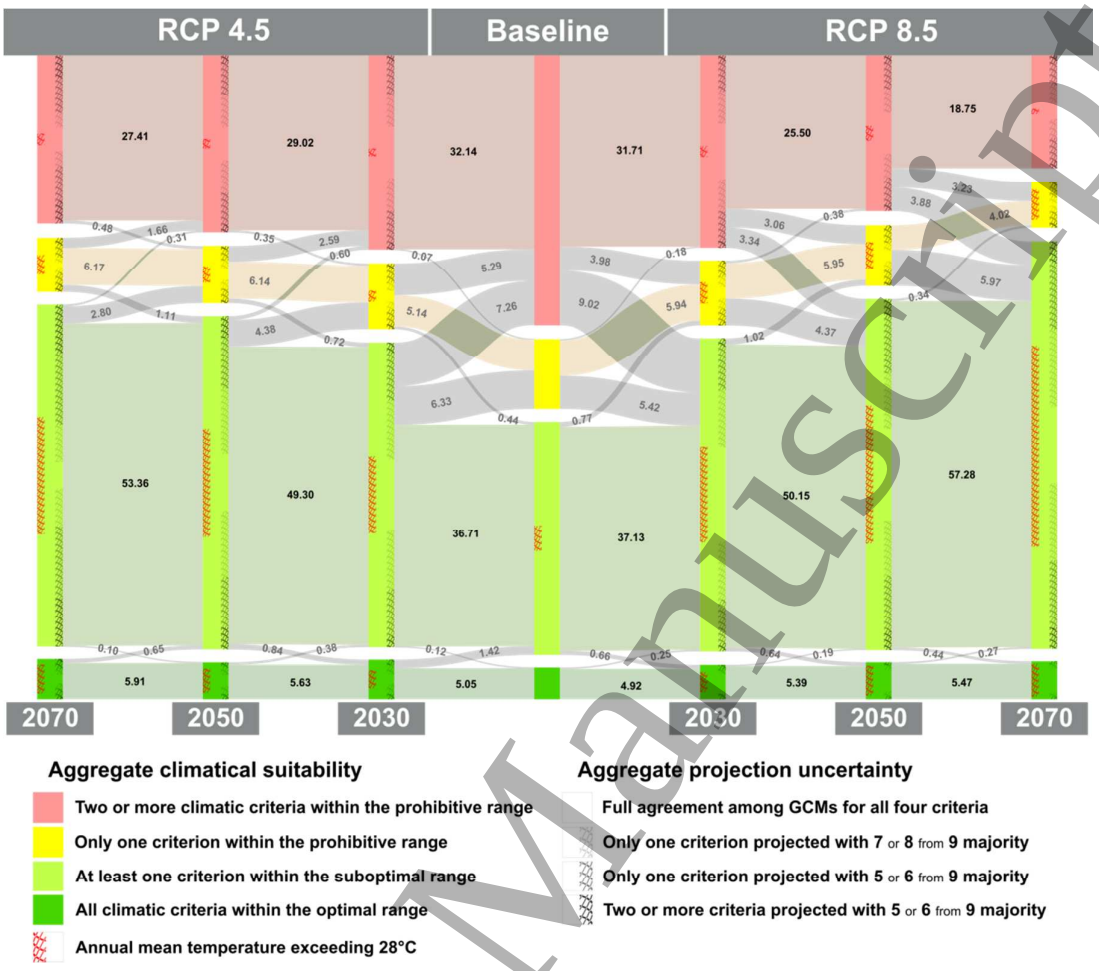

Figure 8 Baseline and projected aggregate climatic suitability dynamics
Baseline (2000) classification and future projections for three time sections under two IPCC AR5 representative concentration pathways 4.5 and 8.5 are reflected proportional (%) to the total investigated area. Inter-nod connections (flows) smaller than 0.05 % are not demonstrated. For more details on the use of Sankey diagrams in illustration of geographic shifts, view the dedicated article: Cuba (2015). Sankey diagram was produced in D3.js JavaScript library (Bostock *et al* 2011) and visually optimized in Inkscape 9.2.

Table 3 Classification agreement between the data simulations and their ensemble at the aggregate level

RCP	Period	Climatic data simulations								
		AC	CC	BC	MP	NO	MG	GF	HE	IP
4.5	2030	90.22	88.27	89.60	85.82	90.66	85.92	78.39	89.99	89.89
	2050	92.48	88.77	92.30	83.26	90.90	85.61	82.34	85.76	89.00
	2070	89.39	93.02	87.31	86.32	88.76	86.11	84.45	81.24	87.45
8.5	2030	92.87	89.35	88.20	90.73	89.27	84.20	84.89	83.19	76.61
	2050	91.20	88.66	87.58	91.69	82.76	87.11	86.60	79.35	74.54
	2070	91.21	88.41	88.57	88.06	83.26	84.48	82.52	78.32	65.90

Resemblance of the aggregate climatic classification by each of the nine simulations used in this study with their ensemble is expressed as proportion (%) of the sum of the areas with matching classification to the total area. Color-code reflects five levels: below 75%, 75 - 80%, 80.1 - 85%, 85.1 - 90% and above 90%. Nine IPCC AR5 simulations of representative concentration pathways RCP 4.5 and RCP 8.5 were used, here abbreviated as AC: ACCESS1.0 (Bi *et al* 2013, Dix *et al* 2013), CC: CCSM4 (Gent *et al* 2011), IP: IPSL-CM5A-LR (Dufresne *et al* 2013), NO: NorESM1-M (Bentsen *et al* 2013), GF: GFDL CM3 (Donner *et al* 2011), BC: BCC_CSM1.1 (Xin *et al* 2013), MG: MRI-CGCM3 (Yukimoto *et al* 2012), MP: MPI-ESM-LR (Giorgetta *et al* 2013) and HE: HadGEM2-ES (Martin *et al* 2011). Each time period corresponds to a 20 year (averaged) time section centered on the mentioned year. GCMs are rank-sorted from left to right by their overall resemblance to ensemble.

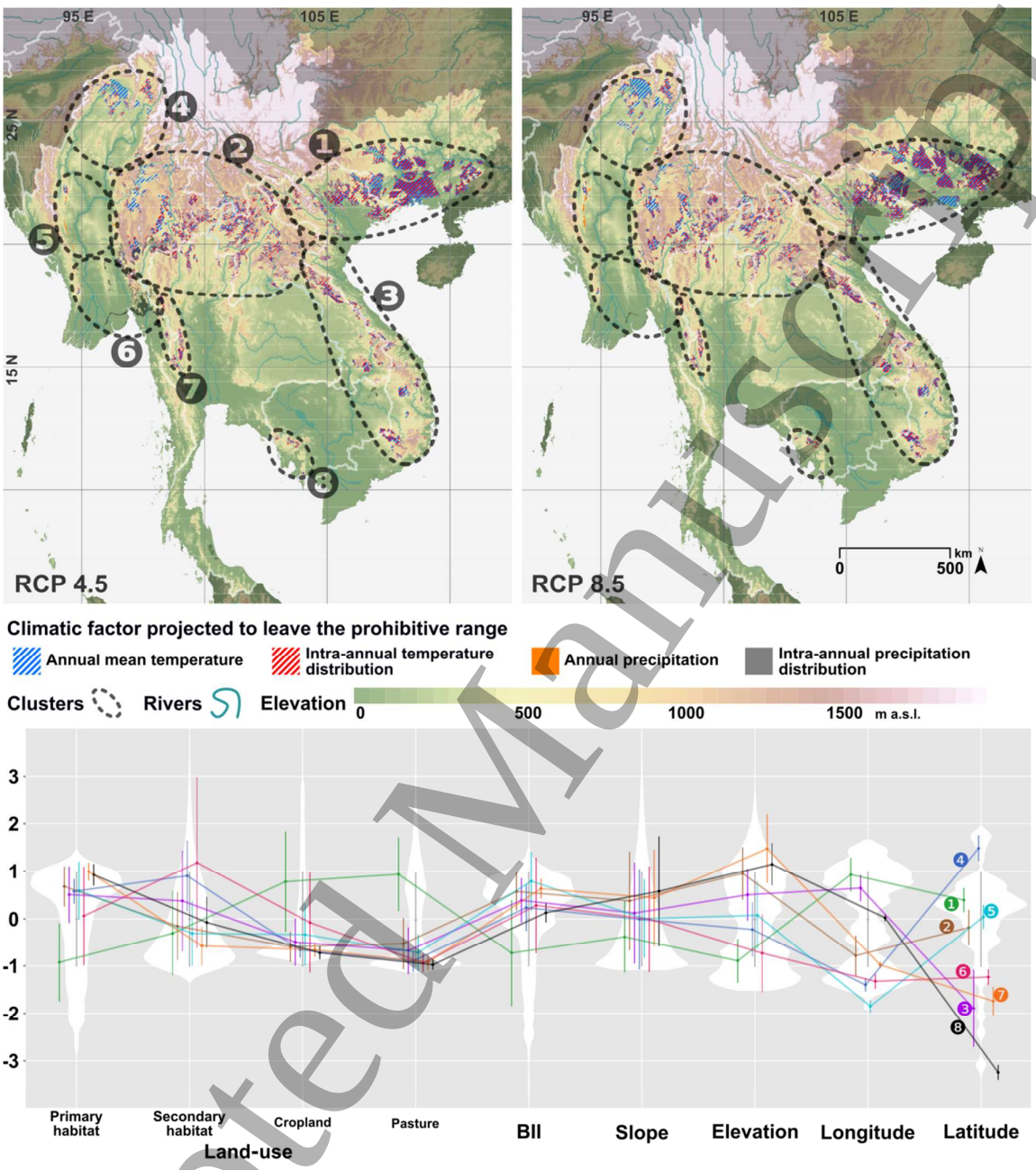

Figure 9 Areas projected with high certainty to become climatically suitable for rubber cultivation by 2030

Land use composition (Hoskins *et al* 2016), physiographic composition (USGS GTOPO30) and biodiversity intactness index (BII) (Newbold *et al* 2016) were used to group the parts of the study area which were projected with high ensemble consensus to become climatically suitable for rubber cultivation into eight clusters using the Grouping Analysis tool of ArcGIS 10.2.2. Violin plots (bottom panel) were generated using the 'ggplot2' 2.1.0 R package and visually optimized in Inkscape 9.2. Terms primary and secondary habitat represent 'undisturbed natural' and 'recovering, previously disturbed natural' habitats respectively. Variables shown above are adjusted to share zero mean and unit variance. For original scale, please see supplementary material figures S4 to S6.

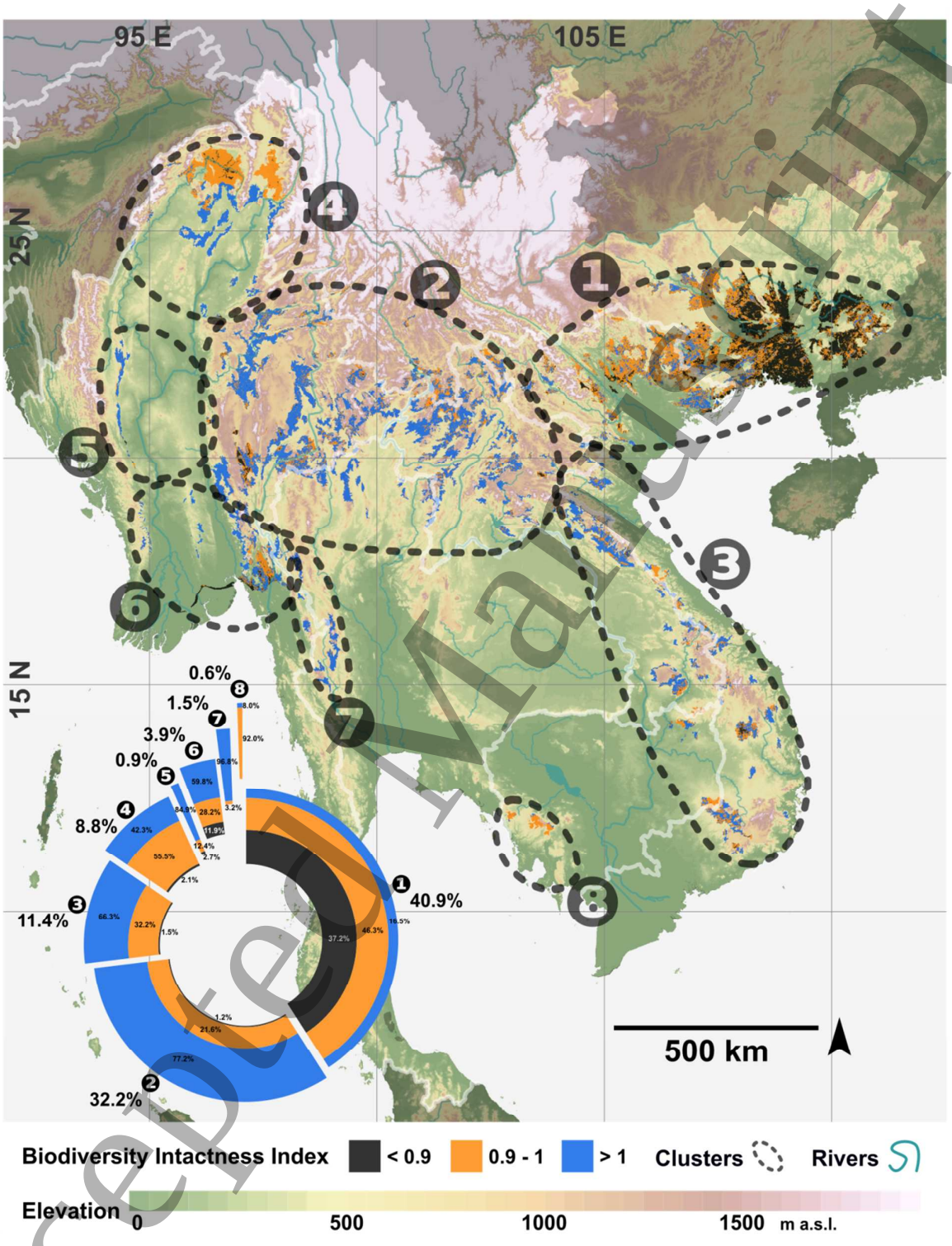

Figure 10 Biodiversity Intactness Index in high certainty shift zones
Biodiversity intactness index (BII) from Newbold *et al* (2016) extracted for Areas projected with high certainty to become climatically suitable for rubber cultivation by 2030. See supplementary material figure S2 for complete frame coverage.

Exposure to excessive heat

Projected exposure to annual mean temperature levels exceeding 28°C in the study area is presented in figure 11. Based on WorldClim data, total baseline area with this characteristic is limited to 14570 km^2 (less than 0.6 % of the total investigated area) located between 12.33 °N, 100°E and 16.33 °N, 101.50 °E in Thailand. Ensemble projections based on 7/9 to 9/9 majority classification suggest that by 2030, under RCP 4.5 this area may increase 25 fold (14.3% of GMS) and 35 fold (20.5% of GMS) under RCP 8.5 stretching northwards to 22°N in the central parts of the Irrawaddy basin. By 2050 however, this criterion may be associated with 23.2% of the total area under RCP 4.5 and 31.2 % under RCP 8.5 increasing respectively by 2070 to 26.5% and 38.9%.

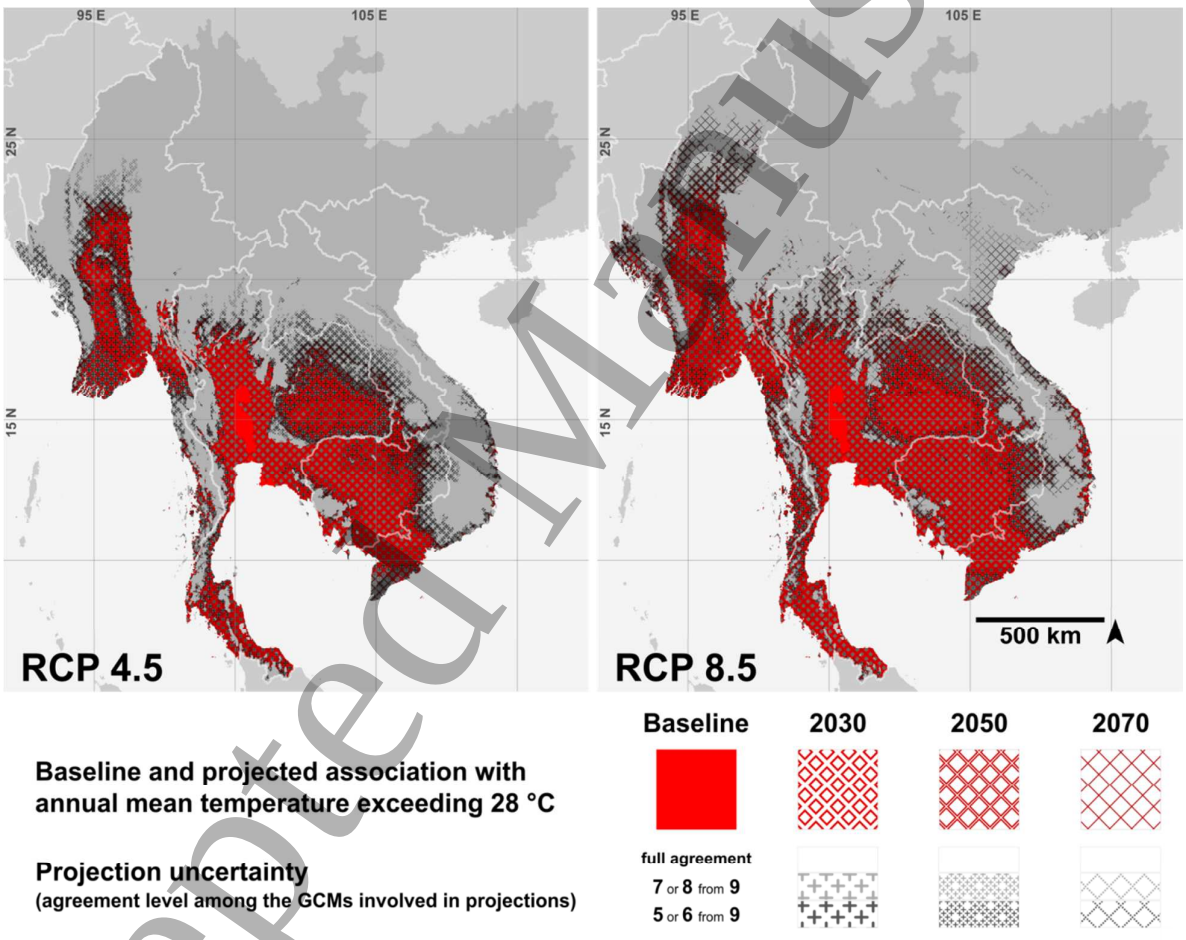

Figure 11 Baseline and projected extent of the exposure to mean annual temperature above 28°C
Each panel contains seven (1+3+3) layers of information: exposure to mean annual temperature above 28°C at the baseline (×1), projected shifts between the four time sections (×3), and the strength of the ensemble majority suggesting the shift/no-shift(×3). Please view this figure in original resolution and consult the usage guide provided in the supplementary material for clarifications.

Discussion

Contrasts and conjunctions with comparable studies

Zomer *et al* (2014) conducted a study focusing on the potential changes in the area conducive to rubber cultivation in Xishuangbanna, Yunnan, China using environmental stratification while averaging all four AR5 RCPs which suggested an increase from 33.5% to 74.5% of the total prefecture area by 2050. Our findings for the same temporal and spatial frame are 52.5% (43.7% with high certainty) under RCP 4.5 and 83.1% (60.1%) under RCP 8.5. Ray *et al* (2016a, 2016b) used MaxEnt ecological niche modeling tool exploring the rubber producing Western Ghats and the North-East regions of India and noted a substantial attachment of the projection outcome to the region used for calibration. If Amazonia was used for model calibration, only a very limited southern part of Western Ghats was returned as suitable by MaxEnt while established rubber growing regions were left out. They observed the same limited transferability pattern while calibrating MaxEnt with each of two Indian rubber producing regions projecting for the other, one at a time. They reached plausible projections only by pooled occurrence points for parameter estimation. Ahrends *et al* (2015) investigated the expansion trends of rubber cultivation in roughly the same geographical frame as this study and concluded that this land use is stretching into increasingly less suitable zones jeopardizing biodiversity and landscape functions. They included a typhoon damage risk assessment based on historical tropical cyclone tracks which, when compared with the area projected with high certainty in this study to become climatically conducive to rubber cultivation by 2030, suggests current typhoon risk zones to overlap only with parts of clusters one (13.2%) and three (2.2%). This overlapping area in cluster one is limited to a 50 km inland buffer of the Guangxi coastline between 106.50°E and 109.66°E. Recent studies on the influence of climate change on western North Pacific tropical cyclone tracks however project reductions in both frequency and intensity of typhoons in future for our area of interest mainly due to northward diversion (Colbert *et al* 2015, Kossin *et al* 2016, Zhang and Wang 2017). Liu *et al* (2015) projected the change in the area with potential for Para rubber cultivation in China covering all five provinces with rubber cultivation background (Hainan, Yunnan, Guangdong, Guangxi and Fujian) using ecological niche modeling to and reported a 15% increase by 2050 from about 400000 km^2 in 2010.

With the exception of cluster 1, which encompasses a major biotically compromised (BII<0.9) area share, most of the regions projected to gain climatic potential for rubber cultivation are chiefly composed of intact primary habitats (figure 10 and supplementary material figure S4). In these areas land use modifications of significant scale require serious attention to the potential impacts on the ecological integrity and ecosystem functions and services. The ongoing improvements in the scientific understanding and practice of concepts such as rubber based agroforestry systems (Langenberger *et al* 2017) and Green rubber eco-certification (Kennedy *et al* 2017) offer promising options for

environmentally friendly rubber cultivation, particularly as support from smallholder side for participation in ecosystem protection appears to grow (Min *et al* 2018, Wigboldus *et al* 2017).

Strengths and limitations of the projection approach

Hevea brasiliensis is not only a plant and therefore a sessile species but also a crop subject to non-natural sources of influence (e.g. breeding and crop management), which may affect the reliability of species distribution models if based on biased presence and pseudo-absence records. From our point of view rule-based models tend to be less prone to circular reasoning but risk engaging non-accurate classification rising from misestimated or dated tolerance thresholds (e.g. due to breeding).

We chose to assign equal weights to the climatic criteria involved in this study, and also to the GCMs forming the ensemble single criteria layers. However, we acknowledge that a non-equal weight approach based on justified quantification of the influence associated with each criterion or its ensemble projection homogeneity (in case of GCMs, based on data quality) is plausible.

Non-climatic factors (e.g. soil conditions, land physiography, labor and market access) which are known to be decisive in suitability for rubber cultivation were not involved in this study. Coverage of a broad range of suitability determining factors in a single study faces serious technical challenges. Different variables can often not be processed with a general approach as the scale relevant for some factors may not necessarily match the scale suitable for the others. The availability and quality of data in a standardized form are also two crucial limiting features. However, some factors relevant in smaller scale (e.g. soil properties) can be nested in those relevant in larger scale (e.g. climatic conditions) by subsequent localized assessments. This requires the provision of the outputs of studies such as this in a modular form exploitable for third parties. The KMZ files accompanying this manuscript do not only provide the findings unchained from resolution loss, but can also be used by future studies as a base to expand upon.

Although recent trajectories of GHG emissions are closest to the RCP 8.5 (supplementary material figure S7), this climate change scenario incorporates some assumptions concerning the use of fossil energy resources which are in the long-run technically improbable (Capellán-Pérez *et al* 2016, Ritchie and Dowlatabadi 2017a, 2017b, Wang *et al* 2017). In view of the concerns and evidence regarding rapid changes in land use and climate, it is counterintuitive to use the early years of the last decade as baseline. Nevertheless, most required underlying data components are being revised not with emphasis on updating but on resolution (e.g. Newbold et al. 2016) or precision (e.g. Fick and Hijmans 2017).

Compared with the lower temperature tolerance limits known for Para rubber, upper thresholds and consequences of exposure to high levels of ambient temperature are not well understood. The global area already exposed to annual mean temperature above 28° C (supplementary material figure S9) does not match typical rubber growing regions. In case of the GMS, a comparison between figures 2

and 11 underlines this point. Mesocosm experiments (Stewart *et al* 2013, Bestion *et al* 2015, Fordham 2015) and other manipulation methods which have recently gained prominence in studies aiming at a better understanding of the responses of the organisms to a warming climate can illuminate the way for *H. brasiliensis* as well.

The methods developed in this article are applied to a relatively restricted case study, rubber cultivation in the GMS. Nevertheless, the potential for transferability to other world regions and other cropping systems is very high, as the vast majority of datasets used is freely available for scientific purposes. The phenological and physiological crop specific background data for other crop plants can be collected from text books and literature reviews. Potential applications that come to mind might be the potential suitability for oil palm plantation systems, coffee agroforestry or bio-economically important crops such as sugar cane and maize and its´ potential northern distribution limits.

In order to broaden the audience of this study and to facilitate the use of its outputs for potential decision makers, we have produced two KMZ files (one for each RCP) which summarize the information behind figures 5, 7 and 11, covering the baseline and the 2030s time windows. These files can easily be loaded in Google Earth™ to check the conditions for a given location by clicking.

Conclusion

Even though the climatic change in the GMS is projected to be predominantly in the direction of higher suitability for rubber cultivation, the expansion of climatically optimal area is projected to be minimal. When including the exposure to annual mean temperatures exceeding 28°C (current estimate of excessive heat for *Hevea* rubber), as a limiting factor, then even a heavy reduction in the total climatically optimal area is likely to occur (see figure 8).

Across the time span investigated in this study (limited to 2070), about half of the new area with climatic potential for rubber cultivation is projected to emerge by 2030, near half of which is ecologically pristine (see figure 10). This pattern, in combination with factors encouraging rubber cultivation in higher altitudes and latitudes underscores the urgency and importance of careful future land use planning. Local and regional decision-makers can use mid- to (more cautiously) long-term assessment such as this to develop policy guidelines and decision support mechanism that can take the occurrence of potential new land use and land management systems into account. Either to prepare a certain region for potential innovations regarding the demands to local infrastructure, or to put necessary guidelines and rules into place to “soften the blow” these innovations might have on traditional systems or biodiversity and nature conservation.

Acknowledgements

The authors want to thank the German Ministry of Science and Technology for supporting the research that led to this publication under the LILAC and SURUMER projects (grant numbers FKZ 0330797A

and FKZ 01 LL 0919) as well as for funding its open access publication. We deeply appreciate the raw data provision by all sources mentioned in this article. We are grateful to Kevin Thellmann, Benjamin Warth and the anonymous referees for their constructive criticisms and insights which helped us improve an earlier draft of this paper.

Author Contributions

R.G. conceived, designed and conducted the study. R.G., M.C. and J.S. prepared the manuscript.

Competing Interests: The authors declare they have no competing interests.

References

Abd Karim Y 2008 Static modelling approaches to predict growth (girth) of Hevea brasiliensis as tools for extension activities in Malaysia *J. Rubb. Res.* **11** 171–86

Ahrends A, Hollingsworth P M, Ziegler A D, Fox J M, Chen H, Su Y and Xu J 2015 Current trends of rubber plantation expansion may threaten biodiversity and livelihoods *Global Environ.Change* **34** 48–58

Beckschäfer P 2017 Obtaining rubber plantation age information from very dense Landsat TM & ETM + time series data and pixel-based image compositing *Remote Sens.Environ.* **196** 89–100

Bestion E, Teyssier A, Richard M, Clobert J and Cote J 2015 Live Fast, Die Young: Experimental Evidence of Population Extinction Risk due to Climate Change *PLOS Biology* **13** e1002281

van Beilen J B and Poirier Y 2007a Establishment of new crops for the production of natural rubber *Trends Biotechnol.* **25** 522–9

van Beilen J B and Poirier Y 2007b Guayule and Russian dandelion as alternative sources of natural rubber *Crit.Rev.Biotechnol.* **27** 217–31

Bentsen M *et al* 2013 The Norwegian Earth System Model, NorESM1-M – Part 1: Description and basic evaluation of the physical climate *Geosci.Model Dev.* **6** 687–720

Berger A, Yin Q, Nifenecker H and Poitou J 2017 Slowdown of global surface air temperature increase and acceleration of ice melting *Earth's Future* **5** 811–22

Bi D *et al* 2013 The ACCESS coupled model: Description, control climate and evaluation *Aust.Meteorol.Oceanogra.J.* **63** 41–64

Bostock M, Ogievetsky V and Heer J 2011 D3: data-driven documents *IEEE Trans.Visual.Comput.Graphics* **17** 2301–9

Capellán-Pérez I, Arto I, Polanco-Martínez J M, González-Eguino M and Neumann M B 2016 Likelihood of climate change pathways under uncertainty on fossil fuel resource availability *Energy Environ.Sci.* **9** 2482–96

Chen B *et al* 2016a Mapping tropical forests and deciduous rubber plantations in Hainan Island, China by integrating PALSAR 25-m and multi-temporal Landsat images *International Journal of Applied Earth Observation and Geoinformation* **50** 117–30

Chen H, Yi Z-F, Schmidt-Vogt D, Ahrends A, Beckschäfer P, Kleinn C, Ranjitkar S and Xu J 2016b Pushing the limits: The pattern and dynamics of rubber monoculture expansion in Xishuangbanna, SW China *PLoS ONE* **11**

Colbert A J, Soden B J and Kirtman B P 2015 The impact of natural and anthropogenic climate change on western North Pacific tropical cyclone tracks *J.Clim.* **28** 1806–23

Collins M *et al* 2013 Long-term climate change: projections, commitments and irreversibility *Climate Change 2013: The Physical Science Basis. Contribution of Working Group I to the Fifth Assessment Report of the Intergovernmental Panel on Climate Change* ed T F Stocker, D Qin, G-K Plattner, M Tignor, S K Allen, J Boschung, A Nauels, Y Xia, V Bex and P M Midgley (Cambridge, United Kingdom and New York, NY, USA: Cambridge University Press) pp 1029–136

Cook J *et al* 2016 Consensus on consensus: a synthesis of consensus estimates on human-caused global warming *Environ. Res. Lett.* **11** 048002

Cornish K 2017 Alternative Natural Rubber Crops: Why Should We Care? *Technology and Innovation* **18** 245–56

Cuba N 2015 Research note: Sankey diagrams for visualizing land cover dynamics *Landsc.Urban Plann.* **139** 163–7

Dix M *et al* 2013 The ACCESS coupled model: Documentation of core CMIP5 simulations and initial results *Aust.Meteorol.Oceanogra.J.* **63** 83–99

Dlugokencky E 2017 Trends in atmospheric methane. *National Oceanic & Atmospheric Administration, Earth System Research Laboratory (NOAA/ESRL), Global Monitoring Division.* Online: https://www.esrl.noaa.gov/gmd/ccgg/trends_ch4/

Dlugokencky E and Tans P 2017 Trends in atmospheric carbon dioxide. *National Oceanic & Atmospheric Administration, Earth System Research Laboratory (NOAA/ESRL), Global Monitoring Division.* Online: https://www.esrl.noaa.gov/gmd/ccgg/trends/global.html

Dong J, Xiao X, Chen B, Torbick N, Jin C, Zhang G and Biradar C 2013 Mapping deciduous rubber plantations through integration of PALSAR and multi-temporal Landsat imagery *Remote Sens.Environ.* **134** 392–402

Dong J, Xiao X, Sheldon S, Biradar C and Xie G 2012 Mapping tropical forests and rubber plantations in complex landscapes by integrating PALSAR and MODIS imagery *ISPRS J.Photogramm.Remote Sens.* **74** 20–33

Dong N, McMahan C M, Whalen M C, Cornish K and Coffelt T A 2017 Transgenic guayule for enhanced isoprenoid production

Donner L J *et al* 2011 The dynamical core, physical parameterizations, and basic simulation characteristics of the atmospheric component AM3 of the GFDL global coupled model CM3 *J.Clim.* **24** 3484–519

Dufresne J-L *et al* 2013 Climate change projections using the IPSL-CM5 Earth System Model: From CMIP3 to CMIP5 *Clim.Dyn.* **40** 2123–65

Fan H, Fu X, Zhang Z and Wu Q 2015 Phenology-based vegetation index differencing for mapping of rubber plantations using landsat OLI data *Remote Sens.* **7** 6041–58

FAOSTAT 2017 Food and Agriculture Organization of the United Nations Online: http://www.fao.org/faostat/en/#data/QC

Fick S E and Hijmans R J 2017 WorldClim 2: new 1-km spatial resolution climate surfaces for global land areas *Int. J. Climatol* **37** 4302–15

Fordham D A 2015 Mesocosms Reveal Ecological Surprises from Climate Change *PLOS Biology* **13** e1002323

Gent P R *et al* 2011 The community climate system model version 4 *J.Clim.* **24** 4973–91

Giorgetta M A *et al* 2013 Climate and carbon cycle changes from 1850 to 2100 in MPI-ESM simulations for the Coupled Model Intercomparison Project phase 5 *Journal of Advances in Modeling Earth Systems* **5** 572–97

Golbon R, Ogutu J O, Cotter M and Sauerborn J 2015 Rubber yield prediction by meteorological conditions using mixed models and multi-model inference techniques *Int.J.Biometeorol.* **59** 1747–59

Grogan K, Pflugmacher D, Hostert P, Kennedy R and Fensholt R 2015 Cross-border forest disturbance and the role of natural rubber in mainland Southeast Asia using annual Landsat time series *Remote Sens.Environ.* **169** 438–53

Hansen M C *et al* 2013 High-Resolution Global Maps of 21st-Century Forest Cover Change *Science* **342** 850–3

Häuser I *et al* 2015 Environmental and socio-economic impacts of rubber cultivation in the Mekong region: challenges for sustainable land use. *CAB Reviews: Perspectives in Agriculture, Veterinary Science, Nutrition and Natural Resources* **10**

He P and Martin K 2015 Effects of rubber cultivation on biodiversity in the Mekong Region *CAB Reviews* **10** 1–7

Hijmans R J, Cameron S E, Parra J L, Jones P G and Jarvis A 2005 Very high resolution interpolated climate surfaces for global land areas *Int.J.Climatol.* **25** 1965–78

Hoskins A J, Bush A, Gilmore J, Harwood T, Hudson L N, Ware C, Williams K J and Ferrier S 2016 Downscaling land-use data to provide global 30" estimates of five land-use classes *Ecology and Evolution* **6** 3040–55

IRSG 2017 Statistical summary of world rubber situation *International Rubber Study Group* Online: http://www.rubberstudy.com/statistics

Jayasooryan K K, Satheesh P R, Krishnakumar R and Jacob J 2015 Occurrence of extreme temperature events – A Probable risk on natural rubber cultivation *Journal of Plantation Crops* **43** 218–24

Kennedy S F, Leimona B and Yi Z-F 2017 Making a green rubber stamp: emerging dynamics of natural rubber eco-certification *International Journal of Biodiversity Science, Ecosystem Services & Management* **13** 100–15

Kirtman B *et al* 2013 Near-term Climate Change: Projections and Predictability *Climate Change 2013: The Physical Science Basis. Contribution of Working Group I to the Fifth Assessment Report of the Intergovernmental Panel on Climate Change* ed T F Stocker, D Qin, G-K Plattner, M Tignor, S K Allen, J Boschung, A Nauels, Y Xia, V Bex and P M Midgley (Cambridge, United Kingdom and New York, NY, USA: Cambridge University Press) pp 953–1028

Koedsin W and Huete A 2015 Mapping rubber tree stand age using pléiades satellite imagery: A case study in Thalang District, Phuket, Thailand *Eng.J.* **19** 45–56

Kositsup B, Montpied P, Kasemsap P, Thaler P, Améglio T and Dreyer E 2009 Photosynthetic capacity and temperature responses of photosynthesis of rubber trees (Hevea brasiliensis Müll. Arg.) acclimate to changes in ambient temperatures *Trees - Structure and Function* **23** 357–65

Kossin J P, Emanuel K A and Camargo S J 2016 Past and projected changes in western north pacific tropical cyclone exposure *J.Clim.* **29** 5725–39

Kou W, Liang C, Wei L, Hernandez A J and Yang X 2017 Phenology-Based Method for Mapping Tropical Evergreen Forests by Integrating of MODIS and Landsat Imagery . *Forests* **8** 1–14

Kou W, Xiao X, Dong J, Gan S, Zhai D, Zhang G, Qin Y and Li L 2015 Mapping deciduous rubber plantation areas and stand ages with PALSAR and landsat images *Remote Sens.* **7** 1048–73

Kreuzberger M, Hahn T, Zibek S, Schiemann J and Thiele K 2016 Seasonal pattern of biomass and rubber and inulin of wild Russian dandelion (Taraxacum koksaghyz L. Rodin) under experimental field conditions *European Journal of Agronomy* **80** 66–77

Langenberger G, Cadisch G, Martin K, Min S and Waibel H 2017 Rubber intercropping: a viable concept for the 21st century? *Agroforest Syst* **91** 577–96

Lewandowsky S, Risbey J S and Oreskes N 2016 The "pause" in global warming: Turning a routine fluctuation into a problem for science *Bull.Am.Meteorol.Soc.* **97** 723–33

Li H, Aide T M, Ma Y, Liu W and Cao M 2007 Demand for rubber is causing the loss of high diversity rain forest in SW China *Biodiversity and Conservation* **16** 1731–45

Li P, Zhang J and Feng Z 2015 Mapping rubber tree plantations using a Landsat-based phenological algorithm in Xishuangbanna, southwest China *Remote Sens.Lett.* **6** 49–58

Li Z and Fox J M 2011a Integrating Mahalanobis typicalities with a neural network for rubber distribution mapping *Remote Sens.Lett.* **2** 157–66

Li Z and Fox J M 2012 Mapping rubber tree growth in mainland Southeast Asia using time-series MODIS 250 m NDVI and statistical data *Appl.Geogr.* **32** 420–32

Li Z and Fox J M 2011b Rubber Tree Distribution Mapping in Northeast Thailand *International Journal of Geosciences* **2** 573–84

Liu S, Zhou G, Fang S and Zhang J 2015 Effects of future climate change on climatic suitability of rubber plantation in China *Ying Yong Sheng Tai Xue Bao* **26** 2083–90

Martin G M *et al* 2011 The HadGEM2 family of Met Office Unified Model climate configurations *Geoscientific Model Dev.* **4** 723–57

McSweeney C F, Jones R G, Lee R W and Rowell D P 2015 Selecting CMIP5 GCMs for downscaling over multiple regions *Clim.Dyn.* **44** 3237–60

Medhaug I, Stolpe M B, Fischer E M and Knutti R 2017 Reconciling controversies about the 'global warming hiatus' *Nature* **545** 41–7

Meinshausen M *et al* 2011 The RCP greenhouse gas concentrations and their extensions from 1765 to 2300 *Climatic Change* **109** 213

Min S, Bai J, Huang J and Waibel H 2018 Willingness of smallholder rubber farmers to participate in ecosystem protection: Effects of household wealth and environmental awareness *Forest Policy and Economics* **87** 70–84

Mittermeier R, Robles Gil P, Hoffmann M, Pilgrim J, Brooks T, Goettsch Mittermeier C, Lamoreux J and Fonseca G 2004 *Hotspots Revisited* (Mexico City: CEMEX)

Muggeo V M R 2003 Estimating regression models with unknown break-points *Stat.Med.* **22** 3055–71

Myers N, Mittermeier R A, Mittermeier C G, Fonseca G A B da and Kent J 2000 Biodiversity hotspots for conservation priorities *Nature* **403** 853

Newbold T *et al* 2016 Has Land use pushed terrestrial biodiversity beyond the planetary boundary? A global assessment *Science* **353** 288–91

Nguyen B T and Dang M K 2016 Temperature dependence of natural rubber productivity in the southeastern Vietnam *Ind.Crops Prod.* **83** 24–30

NSO 1994 The forth Thailand agricultural census. *National Statistical Office Thailand.* Online: http://web.nso.go.th/eng/en/stat/agric/cont_e.htm

Priyadarshan P M, Hoa T T T, Huasun H and de Souza Gonçalves P 2005 Yielding potential of rubber (Hevea brasiliensis) in sub-optimal environments *Journal of Crop Improvement* **14** 221–47

Ramirez-Cadavid D A, Cornish K and Michel Jr. F C 2017 Taraxacum kok-saghyz (TK): compositional analysis of a feedstock for natural rubber and other bioproducts *Industrial Crops and Products* **107** 624–40

Ramirez-Villegas J and Jarvis A 2010 Downscaling Global Circulation Model Outputs: The Delta Method, decision and policy analysis working paper no 1. Online: http://www.ccafs-climate.org/downloads/docs/Downscaling-WP-01.pdf

Rasutis D, Soratana K, McMahan C and Landis A E 2015 A sustainability review of domestic rubber from the guayule plant *Ind.Crops Prod.* **70** 383–94

Ray D, Behera M D and Jacob J 2016a Improving spatial transferability of ecological niche model of Hevea brasiliensis using pooled occurrences of introduced ranges in two biogeographic regions of India *Ecological Informatics* **34** 153–63

Ray D, Behera M D and Jacob J 2014 Indian Brahmaputra valley offers significant potential for cultivation of rubber trees under changed climate *Curr.Sci.* **107** 461–9

Ray D, Behera M D and Jacob J 2016b Predicting the distribution of rubber trees (Hevea brasiliensis) through ecological niche modelling with climate, soil, topography and socioeconomic factors *Ecol.Res.* **31** 75–91

Riahi K, Rao S, Krey V, Cho C, Chirkov V, Fischer G, Kindermann G, Nakicenovic N and Rafaj P 2011 RCP 8.5-A scenario of comparatively high greenhouse gas emissions *Clim.Change* **109** 33–57

Ritchie J and Dowlatabadi H 2017a The 1000 GtC coal question: Are cases of vastly expanded future coal combustion still plausible? *Energy Econ* **65** 16–31

Ritchie J and Dowlatabadi H 2017b Why do climate change scenarios return to coal? *Energy* **140** 1276–91

Rivano F, Maldonado L, Simbaña B, Lucero R, Gohet E, Cevallos V and Yugcha T 2015 Suitable rubber growing in Ecuador: An approach to South American leaf blight *Industrial Crops and Products* **66** 262–70

Scholes R J and Biggs R 2005 A biodiversity intactness index *Nature* **434** 45

Semenov M A and Stratonovitch P 2010 Use of multi-model ensembles from global climate models for assessment of climate change impacts *Clim.Res.* **41** 1–14

Senf C, Pflugmacher D, van der Linden S and Hostert P 2013 Mapping rubber plantations and natural forests in Xishuangbanna (Southwest China) using multi-spectral phenological metrics from modis time series *Remote Sens.* **5** 2795–812

Soratana K, Rasutis D, Azarabadi H, Eranki P L and Landis A E 2017 Guayule as an alternative source of natural rubber: A comparative life cycle assessment with Hevea and synthetic rubber *J.Clean.Prod.* **159** 271–80

Steffen W *et al* 2015 Planetary boundaries: Guiding human development on a changing planet *Science* **347** 1259855

Stephens E M, Edwards T L and Demeritt D 2012 Communicating probabilistic information from climate model ensembles-lessons from numerical weather prediction *Wiley Interdiscip Rev.Clim.Change* **3** 409–26

Stewart R I A *et al* 2013 Mesocosm Experiments as a Tool for Ecological Climate-Change Research *Advances in Ecological Research* Global Change in Multispecies Systems vol 48, ed G Woodward and E J O'Gorman (Academic Press) pp 71–181

Thompson R M, Beardall J, Beringer J, Grace M and Sardina P 2013 Means and extremes: Building variability into community-level climate change experiments *Ecol.Lett.* **16** 799–806

Thomson A M *et al* 2011 RCP4.5: a pathway for stabilization of radiative forcing by 2100 *Climatic Change* **109** 77–94

Thorne P 2017 Briefing: Global surface temperature records: an update *Proceedings of the Institution of Civil Engineers - Forensic Engineering* **170** 50–3

Trisasongko B H 2017 Mapping stand age of rubber plantation using ALOS-2 polarimetric SAR data *European Journal of Remote Sensing* **50** 64–76

Wang J, Feng L, Tang X, Bentley Y and Höök M 2017 The implications of fossil fuel supply constraints on climate change projections: A supply-side analysis *Futures* **86** 58–72

Wigboldus S, Hammond J, Xu J, Yi Z-F, He J, Klerkx L and Leeuwis C 2017 Scaling green rubber cultivation in Southwest China—An integrative analysis of stakeholder perspectives *Science of The Total Environment* **580** 1475–82

Xin X, Zhang L, Zhang J, Wu T and Fang Y 2013 Climate change projections over east asia with BBC_CSM1.1 climate model under RCP scenarios *J.Meteorol.Soc.Jpn.* **91** 413–29

Yu H, Hammond J, Ling S, Zhou S, Mortimer P E and Xu J 2014 Greater diurnal temperature difference, an overlooked but important climatic driver of rubber yield *Industrial Crops and Products* **62** 14–21

Yukimoto S *et al* 2012 A new global climate model of the Meteorological Research Institute: MRI-CGCM3: -Model description and basic performance- *Journal of the Meteorological Society of Japan.Ser.II* **90A** 23–64

Zhang C and Wang Y 2017 Projected future changes of tropical cyclone activity over the Western North and South Pacific in a 20-km-Mesh regional climate model *J.Clim.* **30** 5923–41

Ziegler A D, Fox J M and Xu J 2009 The rubber juggernaut *Science* **324** 1024–5

Zomer R J, Trabucco A, Wang M, Lang R, Chen H, Metzger M J, Smajgl A, Beckschäfer P and Xu J 2014 Environmental stratification to model climate change impacts on biodiversity and rubber production in Xishuangbanna, Yunnan, China *Biol.Conserv.* **170** 264–73